Journal of
Mechanical
Science and
Technology

Journal of Mechanical Science and Technology 21 (2007) 1781~1790

Impact of aspect ratio and surface heating on pollutant transport in street canyons

Xiaomin Xie* and Zhen Huang

Key Laboratory for Power Machinery and Engineering of State Education Ministry, Shanghai Jiao Tong University, Shanghai, 200030, China

(Manuscript Received May 7, 2007; Revised August 13, 2007; Accepted August 18, 2007)

Abstract

This paper investigated the impacts of surface heating on pollutant transport and Air Exchange Rate (AER) in street canyons of different aspect ratios (building height H to street width W) using computational fluid dynamic (CFD) technique. Street canyons of H/W varied from 0.1 to 2 were employed in the study. These street-canyon aspect ratios covered a range of basic flow regimes including skimming flow (H/W =1 and 2), wake interference flow (H/W = 0.5), and isolated roughness flow (H/W = 0.1). Different façade/surface heating imposed different influence on the flow field and pollutant transport in street canyons of different H/W. The AER induced by vertical velocity fluctuation $AER_{w'}$ and mean vertical velocity AER_{w}. AER of street canyon with different H/W and different surface heating exhibited their unique characteristics.

Keywords: Stress canyon; Aspect ratio; Surface heating; Pollutant transport; Air Exchange Rate(AER)

1. Introduction

Vehicular exhausts are major sources of air pollutants in urban areas. On top of rapid urbanization and industrialization, the street is one of the most important urban elements where population and traffic density are relatively high. As a result, human exposure to toxic substances and nuisances at street level increases considerably. In the last two decades, numerous investigations have been devoted to elucidate our understanding of wind flow and pollutant transport in urban street canyons [1-4]. The physical layout of street canyons, which includes building geometry, architecture design, and street canyon dimensions, is the major parameter affecting the characteristic wind flow and pollutant transport in street canyons (also known as flow regimes). Its correlation with street-canyon flow regimes has been studied extensively through wind tunnel experiments [5-8], mathematical modeling [2, 9, 10], and full-scale field measurements [4, 11, 12]. For symmetrical building configurations, the flow regimes and the corresponding vortex characteristics can be expressed in terms of H/W [2]. On the other hand, for unsymmetrical building configurations, making use of the parameters $H1/W$ (leeward-building-height-to-street-width ratio) and $H1/H2$ (leeward-to-windward building height ratio), Xie and Huang [13] summarized the characteristics of wind flow and pollutant transport in both symmetrical and asymmetrical street canyons into three flow regimes.

The thermal effect, which is often neglected in urban-scale environmental fluid mechanics, is another important factor affecting street-canyon wind flow and pollutant transport. In urban areas, the thermal effect is mainly introduced by direct solar radiation on building facades and ground surfaces in the daytime

*Corresponding author. Tel.: +86 21 2836 9010, Fax.: +86 21 6407 8095
E-mail address: xiexiaomin@sjtu.edu.cn

that in turn heats up the air in the vicinity. The hot air is then driven upward by buoyancy [14, 15]. Numerical studies of buoyant flow are relatively limited in literature compared with those in isothermal conditions. Sini et al. [2] studied numerically the mechanical-buoyant induced flow in a modeled cavity. They demonstrated that elevated temperature on building facades could markedly influence the air motion and the wind flow structure as well. Recently, Xie and Huang [16, 17] investigated mechanical-buoyant induced wind flow in an isolated street canyon for a full variety of configurations that further supported the importance of buoyancy in street-canyon wind flow and pollutant transport problems. They concluded that the street-canyon wind flow characteristics are functions of the dimensionless parameter Gr/Re^2.

Recently, the concept of air exchange rate (AER) and pollutant exchange rate (PCH) was adopted to study air ventilation and pollutant dilution in street canyons by both the LES [18] and RNG $k-\varepsilon$ turbulence model [19]. They calculated the AER for street canyons in isothermal conditions, and demonstrated that AER could be taken as a quantitative measure to compare the ventilation efficiency of street canyons.

The aim of this paper is to investigate the impact of aspect ratio and surface heating on the wind flow structure and the associated characteristics of pollutant transport in street canyons of different H/W (0.1, 0.5, 1, and 2). Each H/W represents one of the four basic wind flow structures. Different surface-heating scenarios, i.e., heating on ground surface, and building façade, etc., were performed. This paper contrasts the numerical outputs with different scenarios of surface heating and different H/W at a Reynolds number of 12,000 and a temperature difference (between the heated surface and the ambient air) of 6 oC (Gr/Re^2 is then equal to 6.6). The results presented in this paper would be useful to urban planners and engineers working on urban geometry design when natural ventilation and thermal comfort are their key concerns.

2. Mathematical models

2.1 Model introduction

In the current CFD model, the wind direction was prescribed perpendicular to the infinitely long street canyons (axes). As such, the three-dimensional spatial domain could be simplified to a two-dimensional one. The basic unit of an idealized street canyon was formed by two buildings of equal heights H separated with a breadth W. Nine identical street canyons were aligned in a streamwise direction for maintaining fully developed and periodic street-canyon turbulence.

The mathematical model was based on the numerical solution to the governing fluid flow and transport equations, which were derived from the basic conservation and transport principles in incompressible turbulence:

(a) the mass conservation (continuity) equation:

$$\frac{\partial \bar{u}_i}{\partial x_i} = 0 , \tag{1}$$

(b) the momentum conservation (Navier-Stokes) equation:

$$\bar{u}_j \frac{\partial \bar{u}_i}{\partial x_j} = \left(\frac{\rho - \rho_0}{\rho}\right) g_j - \frac{1}{\rho}\frac{\partial \bar{p}}{\partial x_i} + \frac{\partial}{\partial x_j}\left(\upsilon \frac{\partial \bar{u}_i}{\partial x_j} - \overline{u_i" u_j"}\right), \tag{2}$$

and (c) the energy conservation equation:

$$\bar{u}_i \frac{\partial \bar{\theta}}{\partial x_i} + \frac{\partial}{\partial x_i}\overline{u_i"\theta"} = 0 . \tag{3}$$

Air pollutant concentration was calculated by the convection-diffusion equation for a passive and inert scalar:

$$\bar{u}_i \frac{\partial \bar{c}}{\partial x_i} = \frac{\partial}{\partial x_i}\left(\kappa \frac{\partial \bar{c}}{\partial x_i}\right) + S . \tag{4}$$

Carbon monoxide (CO) was used as the hypothetical vehicular exhaust because of its relatively inert chemical behaviors and prolonged resident time in the atmospheric boundary layer. The vehicular exhaust was simulated in the form of a continuous ground-level line source placed along the street centerline.

In this paper, the Renormalized Group (RNG) $k-\varepsilon$ turbulence theory [20] was used to model the broad range of turbulent motions and transport. The

conservation equations for turbulent kinetic energy (k) and dissipation (ε) in the RNG $k-\varepsilon$ turbulence model were

$$\bar{u}_i \frac{\partial k}{\partial x_i} = \frac{\partial}{\partial x_i}\left(\alpha_k \upsilon_{eff} \frac{\partial k}{\partial x_i}\right) + \frac{1}{\rho} P_k + \frac{1}{\rho} G_b - \varepsilon , \quad (5a)$$

$$\bar{u}_i \frac{\partial \varepsilon}{\partial x_i} = \frac{\partial}{\partial x_i}\left(\alpha_k \upsilon_{eff} \frac{\partial \varepsilon}{\partial x_i}\right) + \frac{1}{\rho} C_{\varepsilon 1} \frac{\varepsilon}{k}\left(P_k + C_{\varepsilon 3} G_b\right) - C_{\varepsilon 2} \frac{\varepsilon^2}{k} , \quad (5b)$$

respectively, where

$$G_b = \rho \beta g \frac{\upsilon_t}{\mathrm{Pr}_t} \frac{\partial \bar{\theta}}{\partial x_i} , \quad (6)$$

$$\upsilon_t = C_\mu \frac{k^2}{\varepsilon} , \quad (7)$$

$$P_k = \upsilon_t \times \frac{\partial \bar{u}_i}{\partial x_j}\left(\frac{\partial \bar{u}_i}{\partial x_j} + \frac{\partial \bar{u}_j}{\partial x_i}\right) , \quad (8)$$

and β is the thermal expansion coefficient in the form

$$\beta = \frac{1}{\rho}\left(\frac{\partial \rho}{\partial \bar{\theta}}\right)_p . \quad (9)$$

The turbulence production due to buoyancy was included as long as the thermal effects in street canyons were taken into consideration. The conservation equation for turbulent kinetic energy had an additional term that used to account for the volumetric production rate due to the interaction between gravitational force and density gradient. The modeling constants for the RNG $k-\varepsilon$ turbulence model adopted in this study are summarized in Table 1.

The aforementioned mathematical models were implemented by using the commercial CFD code Fluent [21]. The numbers of cells and nodes in the computational domains (street canyons) of different H/W are tabulated in Table 2. The spatial resolution near solid boundaries was refined so as to resolve the large gradient of near-wall velocity, temperature and pollutant concentration. The velocity profile was defined as a constant U along the inflow boundary. Zero-gradient boundary conditions were prescribed at the top of the domain while no-slip solid boundaries were used to simulate the ground surface and building facades in the lower part of the domain. The governing equations were discretized by using the finite volume method, and the SIMPLE algorithm was used to solve the equations. A schematic diagram of the computational domain and boundary conditions is shown in Fig. 1.

Table 1. Coefficient adopted for different $k-\varepsilon$ turbulence models.

$k-\varepsilon$ turbulence model	C_μ	σ_k	σ_ε	$C_{\varepsilon 1}$	$C_{\varepsilon 2}$	$C_{\varepsilon 3}$
RNG	0.0845	AF	AF	1.42	1.68	AF

Table 2. Computational parameters employed in CFD calculations.

Aspect ratio H/W	Number of cells	Number of nodes
0.1	321,572	324,470
0.5	351,777	353,885
1	225,889	227,547
2	442,263	444,571

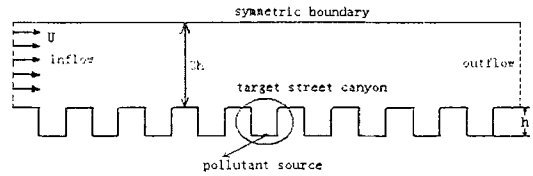

Fig. 1. Computational domain and the boundary conditions.

2.2 Model validation

The accuracy of the CFD model was evaluated by using the extensive experimental database collected from the atmospheric diffusion wind tunnel at the Japanese National Institute for Environmental Studies [22]. Its test section is 2 m high, 3 m wide, and 24 m long. The wind speed range is 0.2-10 ms^{-1}.

Fig. 2(a) depicts the vertical profiles of the dimensionless air temperature along the centerline at Re = 3800. In the core of the street canyon, the current CFD calculated air temperature is slightly lower than the experimental values measured by Uehara et al. [22]. This difference was mainly attributed by the different inflow boundary conditions adopted. In the current CFD model, it was assumed that the horizontal velocity is constant at the inflow boundary, which would influence the roof-level horizontal air speed and temperature profile. Besides, the roughness of the wind tunnel experiment was unknown and that imposed additional uncertainty in our CFD calculation. In the near-ground region, the current CFD calculated temperature is very close to

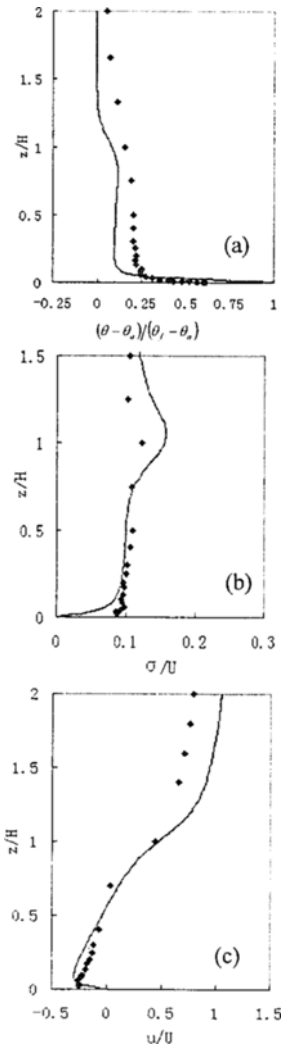

Fig. 2. Vertical profiles of normalized (a) temperature $(\theta-\theta_a)/(\theta_f-\theta_a)$, (b) velocity fluctuation σ /U, and (c) horizontal velocity u/U component along the center line of the street canyon at Re = 3,800. ◆ Measured data [22], —— RNG $k-\varepsilon$ model.

the wind tunnel measurements that computed well the sharp near-ground temperature gradient. Fig. 2(b) illustrates the vertical profiles of the velocity fluctuation along the centerline of the street canyon. The current CFD results agree well with the wind tunnel measurements at the ground level and in the core of the street canyon. The CFD model over-predicts the turbulent kinetic energy at the roof level but converges to the wind tunnel measurements quickly for $z/H \geq 1.5$. Fig. 2(c) compares the dimensionless streamwise velocity along the vertical centerline of the street canyon. The current CFD results agree well with the wind tunnel measurements inside the street canyon. However, the free-stream streamwise velocity at the top of the computational domain is much higher than that of the wind tunnel measured value ($\Delta\, u/U \approx 0.25$). At the roof level, the wind tunnel measurements showed a gentle change in streamwise velocity moving from the street canyon to the upper free-shear layer. Because of the larger free-stream wind velocity, the change in the streamwise velocity calculated by the current CFD model is slightly higher than the wind tunnel measurements.

3. Results and discussion

For a street canyon with different aspect ratios appear different characteristics of flow field and pollutant dispersion in isothermal conditions [2, 4, 13]. For a street canyon of H/W = 1 in isothermal conditions, the wind flow was within the skimming flow (SF) regime of which only one primary vortex was developed in the center core of the street canyon, and the pollutant accumulated in the leeward side. Similar to the one of H/W = 1, the flow in the street

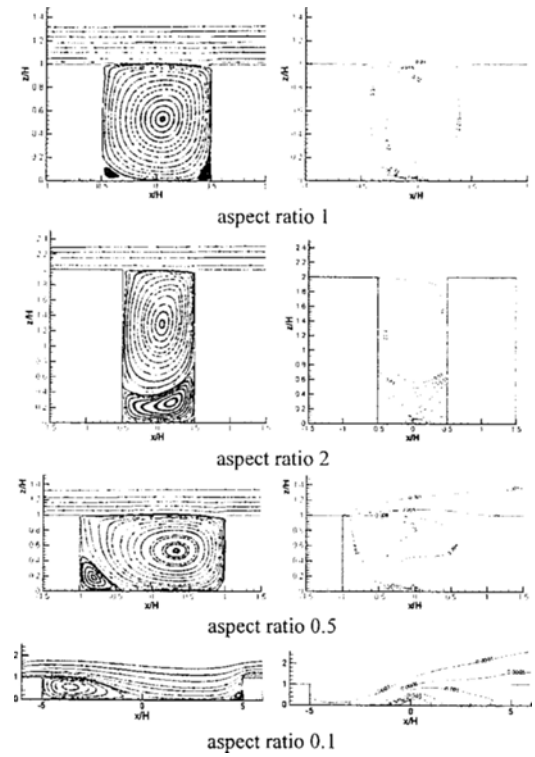

Fig. 3. Flow field and spatial contours of normalized pollutant concentration C/C_0 with different aspect ratio in isothermal condition.

canyon of $H/W = 2$ also lay within the SF regime in which two vertically aligned counter-rotating vortices were developed in isothermal conditions; pollutant at the windward side is higher than that at the windward side. The wind flow in the street canyon of $H/W = 0.5$ falls into the wake interference flow (WIF) regime. With this H/W, a large clockwise-rotating primary vortex together with a small counter-clockwise-rotating secondary vortex (resided at the ground-level leeward corner) were developed; pollutant accumulated at the leeward side because the main vortex. When the street-canyon H/W was further decreased to 0.1, the wind flow became isolated roughness flow (IRF) in which two co-rotating vortices were developed in the street canyon in isothermal conditions. All the results of different aspect ratio in isothermal conditions are shown in Fig. 3.

The thermal energy from building facades or ground surface, which was received from solar radiation, made the air temperature inside street canyon higher than that of the air outside. The elevated air temperature resulted in strong buoyancy in the vicinity of the building facades or the ground surface, which in turn affected the wind flow structure and the pollutant transport behaviors in the street canyons.

3.1 Wind flow structure

In this section, the characteristics of wind flow structure and pollutant dispersion in street canyons of different H/W are discussed. Fig. 4 illustrates the flow field and the corresponding spatial distribution of pollutant in the street canyon of $H/W = 1$.

Upon direct solar radiation, air close to the building facades or the ground surface was hotter than that in the center core of the street canyon. On the other hand, there was a significant temperature depression in region away from the surfaces. For a street canyon of $H/W = 1$ when the sun shone directly into the ground surface and the windward facades, the current CFD outputs showed that the primary vortex was divided into two counter-rotating vortices (Fig. 4). If the leeward building facade was heated up, one main vortex was generated in the canyon, but the vortex was intensified compared with that in the no heated canyon.

In the street canyon of $H/W = 1$, previous studies in isothermal conditions [13] had shown that air pollutants accumulated in the leeward side. However, pollutant accumulation switched from the leeward side to the windward side if ground and windward surface heated. Under this circumstance, the main street-canyon recirculation was no longer dominated by the clockwise-rotating primary vortex. Instead, the secondary counter-clockwise-rotating vortex in the windward side covered the whole windward building height and extended beyond the street center to the leeward side. As a result, air pollutants were carried toward the windward side once emitted from the street center, which then moved upward along the windward building to the roof level. Eventually, most of the air pollutants are removed from the street canyon at the windward roof level while a limited amount re-entered the street canyon in the leeward side. If the leeward building facade was heated up, one intensified vortex was generated in the canyon; pollutant accumulated in the leeward side.

In the street canyon of H/W =2 under temperature stratification, heating up the ground surface broke the lower vortex into two counter-rotating vortices. The anti-clockwise-rotating vortex on the windward side was driven by the clockwise-rotating vortex in the

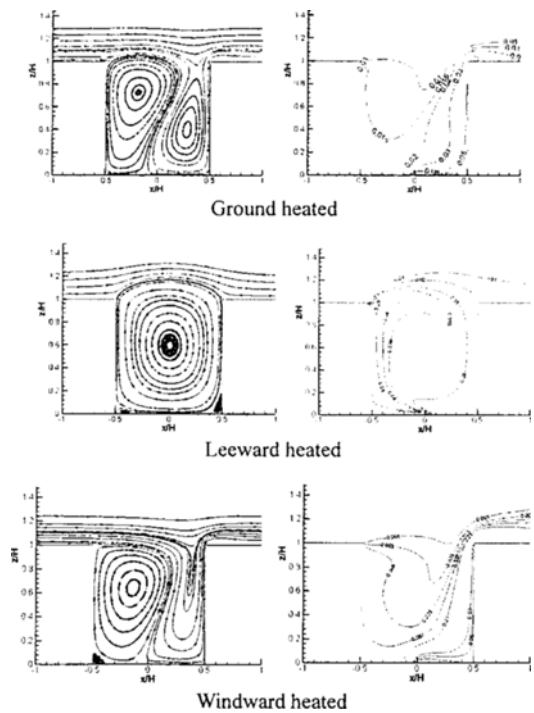

Fig. 4. Flow field and spatial contours of normalized pollutant concentration C/C0 in street canyon with different surfaces heated in aspect ratio 1.

upper part of the street canyon. In contrast, when the leeward building façade was heated up, the air in the vicinity of the leeward building facade was heated up and the hot air rose along this façade; a large single primary vortex was developed covering the whole street canyon. Instead, if the windward building facade was heated up, two vortices were observed in the street canyon, in which the windward vortex was enlarged so that it covered the whole windward building height and held the main volume of the canyon.

In the street canyon of $H/W=2$ under temperature stratification, the current CFD outputs showed that the pollutant accumulated in the leeward side when the ground surface was heated, because one clockwise-rotating vortex covered the pollutant source. When the windward façade was heated, the clockwise-rotating primary vortex extended down to the ground level of street canyon and covered the pollutant source at the street center. Hence, air pollutants were carried by the primary vortex from the street center toward the leeward building and resulted in pollutant accumulation. Whereas, when only the windward facade was heated up, the ground-level pollutant source was covered by the counter-clockwise-rotating secondary vortex. Thus, the air pollutants were transported toward the windward building which caused pollutant accumulation.

As shown in Fig. 6, introduction of windward façade heating led to the formation of a counter-clockwise-rotating vortex at the windward side in the street canyon of $H/W=0.5$. For ground-surface or leeward façade heating, the primary vortex strengthened and extended over the roof level of the street canyon, and one or two tiny vortices developed at the ground-level of windward or leeward.

The pollutant transport behaviors in the street canyon of $H/W=0.5$ were similar regardless of the configurations of street-canyon heating. The vortex structure was dominated by the primary clockwise-rotating vortex which covered the ground-level pollutant line source locating at the street center. Thus, the pollutants were carried toward the leeward side once emitted from the source. Afterward, they were brought upward along the leeward facade and then removed from or re-entered into the street canyon at the roof level.

When the street-canyon H/W was further decreased to 0.1, the vortex at the windward side diminished while the vortex at the leeward side enlarged

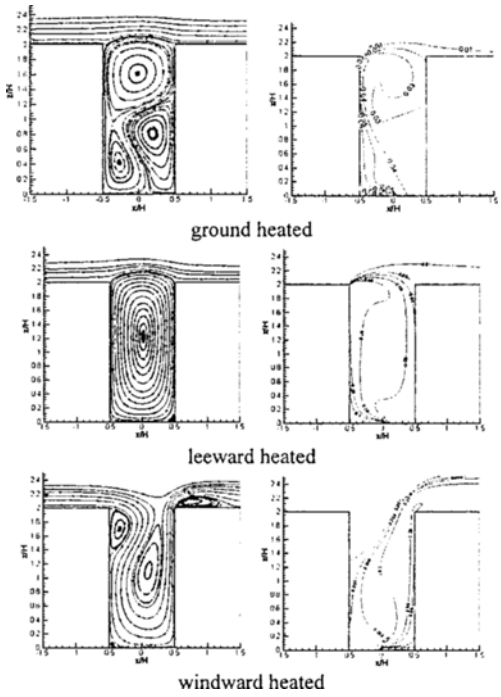

Fig. 5. Flow field and spatial contours of normalized pollutant concentration C/C0 in street canyon with different surfaces heated in aspect ratio 2.

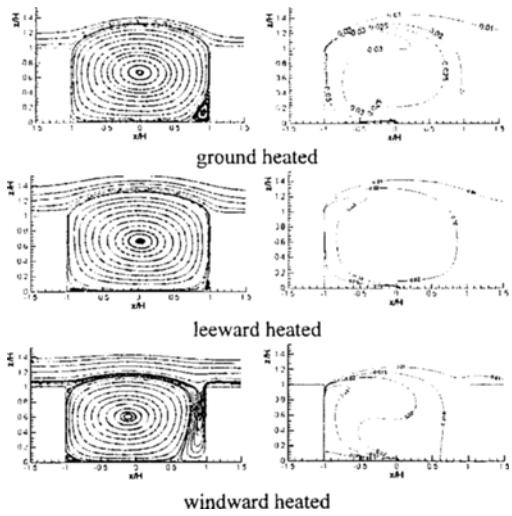

Fig. 6. Flow field and spatial contours of normalized pollutant concentration C/C0 in street canyon with different surfaces heated in aspect ratio 0.5.

further not only in the case of ground surface heating but also in the case of windward facade heating. When leeward façade was heated, two vortices in the canyon enlarged at the same time, and the leeward

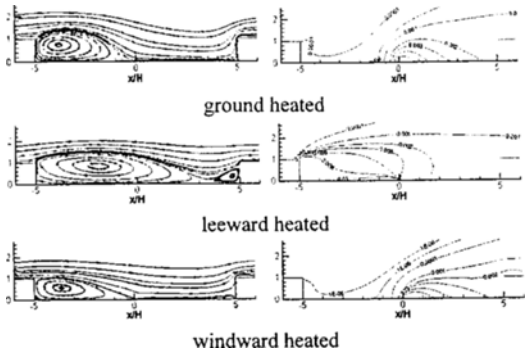

Fig. 7. Flow field and spatial contours of normalized pollutant concentration C/C0 in street canyon with different surfaces heated in aspect ratio 0.1.

side one held the majority volume of the canyon.

Determined by the wind flow, pollutant concentrations in the leeward side were higher than that in the windward side for the street canyon of $H/W = 0.1$ for ground surface and windward facade heating. But pollutant concentrations in the windward side was higher than that in the leeward side when leeward facade heating. This is the reason that the vortex at leeward side covered the ground-level pollutant line source located at the street center, and carried the pollutants to the leeward side once emitted from the source.

3.2 Air exchange rate (AER)

The concept of AER used in street-canyon airflow problems, which represents the volumetric air exchange per unit time within the street canyon, is detailed in Li et al. [19] and Liu et al. [18]. Positive AER (AER+) represents removal of air from the street canyon to the free surface layer, while negative AER (AER-) represents entry of air from the free surface layer into the street canyon. The magnitudes of AER+ and AER- are equal because of mass conservation. The temporal average of positive AER is obtained by integrating the time-dependent AER + (t) along the air ventilation boundary (a line in the current 2D case) $\Gamma = b$ across the street in the following format

$$\begin{aligned}\overline{AER+} &= \int_0^T AER+(t)dt \\ &= \int_0^T \int_\Gamma \left[\overline{w_+}(t,\Gamma) + w''_+(t,\Gamma)\right]_{roof} d\Gamma dt \\ &= \int_\Gamma \left(\int_0^T \left[\overline{w_+}(t,\Gamma) + w''_+(t,\Gamma)\right]_{roof} dt \right) d\Gamma ,\end{aligned} \tag{10}$$

where $\overline{w_+}(t,\Gamma)$ and $w'_+(t,\Gamma)$ are the mean positive vertical velocity and positive vertical velocity fluctuation, respectively. The integral $\int_0^T \left[\overline{w_+}(t,\Gamma) + w'_+(t,\Gamma)\right]_{roof}$ dt is the ensemble average of positive roof-level vertical velocity. It is noteworthy that the removal and entry of air induced by vertical velocity fluctuation are transient processes that cannot be resolved in the current $k-\varepsilon$ turbulence model. Hence, it is assumed that the transient air exchange is divided evenly into removal and entry processes. Moreover, the amount of air removal is equal to entry counterpart. The AER+ can then be determined in accordance with

$$\overline{AER+} = \int_\Gamma \overline{w_+}\big|_{roof} d\Gamma + \frac{1}{2}\int_\Gamma \overline{w''w''}^{1/2}\big|_{roof} d\Gamma . \tag{11}$$

Isotropic turbulence ($u'' = v'' = w''$), a reasonable approximation in the present high-Reynolds-number flow using $k-\varepsilon$ turbulence model, was assumed in this study. The wind tunnel results of Kastner-Klein et al. [6] also suggested isotropy in the street-canyon airflow at such high Reynolds number. Thus,

$$k = \left(\overline{u''u''} + \overline{v''v''} + \overline{w''w''}\right)/2 = 3\overline{w''w''}/2 \tag{12}$$

$$\overline{w''w''}^{1/2}\Big|_{roof} = \sqrt{\frac{2}{3}k}\Big|_{roof} \tag{13}$$

$$\overline{AER+} = \int_\Gamma w_+ d\Gamma + \frac{1}{\sqrt{6}}\int_\Gamma \sqrt{k}\big|_{roof} d\Gamma = AER_w + AER_{w'} \tag{14}$$

The AER values are non-dimensionalized by the volume of street canyon of unity aspect ratio V and the reference time scale T ($= H/u_0$).

Table 3 present the dimensionless AER induced by mean vertical velocity AER_w, vertical velocity fluctuation $AER_{w'}$ and the total AER (AER= AER_w+ $AER_{w'}$) that includes vertical velocity generated and vertical velocity fluctuation generated respectively.

The AER values for the street canyons of V=1 are least compared with the other aspect ratios. AER value of V=1 with leeward heated is larger than that of the other two heated surfaces; this is the reason that characteristics of vortex have obviously changed and vertical air exchange at the top level of the canyon strengthened when leeward heated. Similar with a street canyon of V=1, an AER value of V=2 with leeward heating is larger than that of the other two heated surfaces. But the differences between AER

Table 3. The dimensionless AER induced by mean vertical velocity AER_w, vertical velocity fluctuation $AER_{w'}$ and the total AER.

Ratio	AER	Heated surface		
		Ground	Leeward	Windward
1	AER_w	0.059	0.152	0.061
	$AER_{w'}$	0.091	0.073	0.071
	AER	0.150	0.225	0.132
2	AER_w	0.060	0.162	0.198
	$AER_{w'}$	0.158	0.121	0.083
	AER	0.218	0.283	0.281
0.5	AER_w	0.709	0.586	0.290
	$AER_{w'}$	0.432	0.292	0.468
	AER	1.141	0.878	0.758
0.1	AER_w	8.312	3.478	3.027
	$AER_{w'}$	21.420	11.727	8.592
	AER	29.732	15.205	11.619

values of different heated surfaces have a visible reduction compared with cases of V=1. With aspect ratio V=0.5 and 0.1, the AER values of the street canyon with ground heating are larger than that of leeward and windward heating. In the cases of aspect ratio V=0.5 and 0.1, the ground have a larger area than building surfaces, and ground heated have a great influence on air exchange and pollutant dispersion, especially in the case of aspect ratio equal to 0.1. Xie et al. [23] concluded that the AER can be estimated by the dimensionless parameter Gr/Re^2 when the bottom of the street canyon is heated and the aspect ratio equal to 1. From this study, it can be found that AER with different heated surfaces is varied. Further study about the relationship between AER and Gr/Re^2 with different heated surface and aspect ratio should be carried out.

4. Conclusions

The CFD results discussed in this paper show that building-facade and ground-surface heating lead to a strong buoyant force close to the surfaces receiving direct solar radiation. The surface heating eventually affects the air exchange between the street canyon and the free-surface layer aloft. The buoyancy induced wind flow combines with the mechanically induced wind flow formed in the street canyon. The flow characteristics are different in the street canyon of different H/W in isothermal conditions. Similarly, different façade/surface heating imposes different influence on the flow field and pollutant transport in street canyons of different H/W. For $H/W=1$ (the basic flow structure was SF with one primary vortex in the street canyon), two counter-rotating vortices were developed for ground and leeward surface heating. Because of the stronger vortices in the windward side, the pollutant concentration in the leeward side was higher than that in the windward side. When the windward was heated, there was one main vortex in the canyon, so the pollutant accumulated in the leeward side. At $H/W=2$ (the basic flow structure was SF with two counter-rotating vortices in the street canyon), one primary vortex was developed in the street canyon and air pollutant accumulated on the leeward side when the leeward building facade was heated. Several vortices were developed in the street canyon when the windward and ground was heated; pollutant transport depended on the characteristics of vortices within the street canyon. At $H/W=0.5$ (the basic flow structure was WIF with one primary vortex and a tiny secondary vortex in the street canyon); one primary vortex was developed in the street canyon with different surface heating, and air pollutant accumulated at the leeward side. At $H/W=0.1$ (the basic flow structure was IRF with two same rotating vortices in the street canyon); one main clockwise-rotating vortex was developed in the leeward side of street canyon for ground and windward side heating, and the air pollutant was transported not only by this primary vortex but also by the wind flow over the ground directly. The vortex in the leeward side enlarged, pollutant dispersion was mainly influenced by this vortex, and pollutant was accumulated at the leeward side when the leeward heated. The AER values for the street canyons were markedly affected by buoyancy force. The AER induced by vertical velocity fluctuation $AER_{w'}$ and mean vertical velocity AER_w. AER of street canyon with different H/W and different surface heating exhibited their own unique characteristics.

Acknowledgements

This project is supported by China Postdoctoral Science Foundation (No. 20060400647). The authors would like to thank Dr. Dennis Y. C. Leung of Hong Kong University and Dr. Chun-Ho Liu of Hong Kong

Polytechnic University for their contributions to this research.

Nomenclature

$\bar{c}$: Pollutant concentration (g m-3)
g : Acceleration due to gravity (m sec-2)
Gr : Grashof number $Gr = \frac{\beta g \Delta\Theta H^3}{\upsilon^2}$
H : Height of the buildings (m)
$H1$: Height of the leeward building (m)
$H2$: Height of the windward building (m)
Re : Reynolds number $\mathrm{Re} = \frac{U H_1}{\upsilon}$
Ri : Bulk Richardson number $\mathrm{Ri} = \frac{gH(\theta_n - \theta_f)}{\theta_n u_0^2}$
S : Pollutant source strength
$\underline{U}$: Ambient wind speed (m sec-1)
$\bar{u}_i = (\bar{u}, \bar{v}, \bar{w})$: Velocity tensors in the (x, y, z) directions (m sec-1)
$u_i' = (u', v', w')$: Velocity fluctuation tensors in the (x, y, z) directions (m sec-1)
W : Width of the street (m)
$\Delta\Theta$: Temperature difference $\Delta\Theta = \Theta_f - \Theta_n$
κ : Molecular diffusivity
υ : Molecular kinematic viscosity
$\bar{\theta}$: Air temperature (°C)
Θ_n : Ambient air temperature (°C)
Θ_f : Surface temperature (°C)

References

[1] I. Eliasson and B. Offerle, Wind fields and turbulence statistics in an urban street canyon, *Atmospheric Environment.* 40 (2006) 1-16.
[2] J. F. Sini, Pollution dispersion and thermal effects in urban street canyon, *Atmospheric Environment.* 30 (1996) 2659-2677.
[3] X. Xie, Z. Huang, J. S. Wang and Z. Huang, Impact of building configuration on Air Quality in street canyon, *Atmospheric Environment.* 36 (2005) 3601-3613.
[4] T. R. Oke, Street design and urban canopy layer climate, *Energy and Building.* 11(1988) 103-131.
[5] C. J. Baker and D. M. Hargreaves, Wind tunnel evaluation of a vehicle pollution dispersion model, *Journal of wind Engineering and industrial Aerodynamics.* 89 (2001) 187-200.
[6] P. Kastner-Klein and E. J. Plate, Wind-tunnel study of concentration fields in street canyons, *Atmospheric Environment.* 33 (1999) 3973-3979.
[7] P. Kastner-Klein and E. Fedorovich, A wind tunnel study of organized and turbulent air motions in street canyons, *Journal of Wind Engineering and Industrial Aerodynamics.* 89 (2001) 849-861.
[8] R. N. Meroney and M. Pavageau, Study of line source characteristic for 2-D physical modeling of pollutant dispersion in street canyons, *Journal of wind Engineering and Industrial Aerodynamics.* 62 (1996) 37-56.
[9] T. L. Chan and G. Dong, Validation of a two-dimensional pollutant dispersion model in an isolated street canyon, *Atmospheric environment.* 36 (2002) 861-872.
[10] J. Y. Xia and D. Y. C. Leung, Pollutant dispersion in urban street canopies, *Atmospheric Environment.* 35 (2001) 2033-2043.
[11] R. Berkowicz, Using measurements of air pollution in streets for evaluation of urban air quality-meteorological analysis and model calculations, *The Science of the Total environment.* 189/190 (1996) 259-265.
[12] B. Croxford, Siting considerations for urban pollution monitors, *Atmospheric Environment.* 32 (1998) 1049-1057.
[13] X. Xie, Z. Huang, J. S. Wang and Z. Huang, The impact of urban street layout on local atmospheric environment, *Building and Environment.* 41 (2006) 1352-1363.
[14] J. J. Kim and J. J. Baik, Urban street-canyon flows with bottom heating, *Atmospheric Environment.* 35 (2001) 3395-3404.
[15] P. Louka and G. Vachon, Thermal effects on the airflow in a street canyon-nantes '99 experimental results and model simulation, The 3rd international conference on Urban Air Quality-Loutraki (2001) 19-23.
[16] X. Xie, Z. Huang, J. S. Wang, and Z. Xie, The impact of solar radiation and street layout on pollutant dispersion in street canyon, *Building and Environment.* 40 (2005) 201-212.
[17] X. Xie, Z. Huang and J. S. Wang, Thermal effects on vehicle emission dispersion in an urban street canyon, *Transportation Research Part D: Transportation and Environment.* 10 (2005) 197-212.
[18] C.-H. Liu and D. Y. C. Leung, and M. C. Barth, On the prediction of air and pollutant exchange rates in street canyons of different aspect ratios using large-eddy simulation, *Atmospheric Environment.* 39 (2005) 1567-1574.

[19] X.-X. Li, C.-H. Liu and D. Y. C. Leung, Development of a model for the determination of air exchange rates for the street canyon, *Atmospheric environment* 39 (2005) 7285-7296.

[20] V. Yakhot, S. A. Orszag, Renormalization group analysis of turbulence, *Journal of Scientific Computing*. 1 (1986) 1-51.

[21] Fluent, Fluent home page, http://www.fluent.com (2006)

[22] K. Uehara and S. Murakami, Wind tunnel experiments on how thermal stratification affects flow in and above urban street canyons, *Atmospheric Environment*. 34 (2000) 1553-1562.

[23] X. Xie, C.-H. Liu and D. Y. C. Leung, Characteristics of air exchange in a street canyon with ground heating, *Atmospheric environment, inpress* (2006).